

Bifurcation phenomena of the Generalized Chua's Circuit Through Harmonic Balance Analysis

F. Acar Savacı* and Serkan Günel**

*İzmir Institute of Technology,
Dept. of Electrical and Electronics Eng.,
Gülbahçe, Urla, İzmir, TURKEY

**Dokuz Eylül University,
Dept. of Electrical and Electronics Eng.,
Tınaztepe Kampüsü,
Kaynaklar, Buca, İzmir, TURKEY

Email: serkan.gunel@eee.deu.edu.tr, acarsavaci@iyte.edu.tr

Abstract—In this paper, the harmonic balance analysis of Generalized Chua's circuit exhibiting n-scroll attractors has been accomplished using the dual-input describing functions of the piecewise linear characteristics of the Chua's diode.

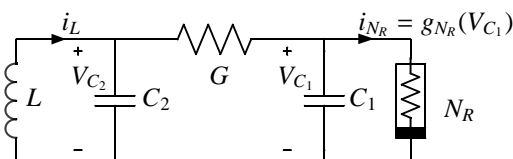


Figure 1: The Chua's Circuit

1. Introduction

The Chua's circuit is one of the systems for which chaos has been verified analytically [1]. Despite its minimal structure, it has a rich diversity of behaviors ranging from equilibrium states to period doubling bifurcations, from quasi-periodicity to intermittency which makes it a milestone in nonlinear research [5]. The rich diversity of dynamical behavior of the circuit given by is experimentally verified [4].

It had been proposed that the double scroll behavior characteristic to the circuit is due to the interacting limit cycles and unstable equilibrium[3]. The existence of interacting predicted limit cycles and unstable equilibrium can be verified using heuristic harmonic balance method. In this method, the circuit is represented in the Luré form first. Then, the output of the linear part is approximated with a limit cycle, and the amplitude and the bias of the nonlinearity are approximated using the the describing functions [2]. The existence of the predicted limit cycles interacting with the equilibrium for the basic form of the circuit with two break points had been verified previously [7, 12].

The Chua's circuit can be generalized in the sense that the number and the position of the scrolls are altered without increasing the dimensionality of the system by modification of the nonlinearity of the circuit [8–11, 13, 14].

In this paper, the harmonic balance analysis of the Generalized Chua's circuit exhibiting n-scroll attractors has been accomplished, by extending the study in [12].

2. The Generalized Chua's Circuit

The Chua's circuit depicted in Fig. 1 has the following state space representation

$$\begin{aligned} \dot{\mathbf{x}} &= \mathbf{A} \cdot \mathbf{x} + \mathbf{b} \cdot \phi(y) \\ y &= \mathbf{C} \cdot \mathbf{x} \end{aligned} \quad (1)$$

where

$$\begin{aligned} \phi(y) &= m_i y + k_i, \quad S_i < y \leq S_{i+1}, \quad S_0 = 0 \\ k_0 &= 0, \quad k_i = \sum_{j=1}^i (m_{j-1} - m_j) S_j \quad i = \pm 1, \pm 2, \dots \end{aligned} \quad (2)$$

$$\mathbf{A} = \begin{pmatrix} -\alpha(1 + \delta) & \alpha & 0 \\ 1 & -1 & 1 \\ 0 & -\beta & 0 \end{pmatrix}, \mathbf{b} = \begin{pmatrix} -\alpha \\ 0 \\ 0 \end{pmatrix} \text{ and } \mathbf{C} = \begin{pmatrix} 1 & 0 & 0 \end{pmatrix} \quad (3)$$

where α , β and δ can be defined in terms of the circuit parameters.

The double scroll, the strange attractor of the Chua's circuit, can be obtained for some specific range of parameters and with two break-points piecewise linear resistor in the circuit. The n-scroll (n=1,2,...) attractor family was obtained as a result of generalization of the Chua's circuit with additional break points in the nonlinear characteristic of the Chua's diode [8]. Due to the generalization of the nonlinear characteristics, it has been shown that increasing the number of scrolls in all state variable directions is also possible [11].

3. Harmonic Balance Analysis

In order to analyze the circuit by harmonic balance method the equations are first written in the classical Lur'e form. The nonlinear part of the Lur'e form of Chua's circuit is as in (2) and the linear part can be represented as,

$$L(s) = \frac{-\alpha(s^2 + s + \beta)}{s^3 + (1 + \alpha(1 + \delta))s^2 + (\beta + \alpha\delta)s + \alpha\beta(1 + \delta)} \quad (4)$$

Assume that the output of the system (1) is

$$y(t) = A + B \sin(\omega t) \quad (5)$$

then the corresponding nonlinearity output is approximately given by

$$\phi(y(t)) \approx N_0(A, B)A + N_1(A, B)B \sin(\omega t) \quad (6)$$

where the approximating gain to the bias input is

$$N_0(A, B) = \frac{1}{\pi} \int_{-\infty}^{\infty} \phi(A + B \sin(\omega t)) dt, \quad (7)$$

and the approximating gain to the sinusoidal input is

$$N_1(A, B) = \frac{1}{2\pi} \int_{-\infty}^{\infty} \phi(A + B \sin(\omega t)) \sin(\omega t) dt. \quad (8)$$

If $\phi : R \rightarrow R$ is memoryless, time invariant and odd with respect to its argument, then both *dual input describing functions* (DIDF), $N_0 : R^2 \rightarrow R$ and $N_1 : R^2 \rightarrow R$ are independent of ω .

The approximation given in (6) valid if

$$|L(j\omega)| \gg |L(jk\omega)|, \quad k = 2, 3, \dots, \quad j^2 = -1 \quad (9)$$

hence the higher order harmonics generated by the nonlinearity can be neglected.

In order to have a limit cycle in the form of (5), the following equations must be satisfied

$$1 + N_0(A, B)L(0) = 0 \quad (10a)$$

$$1 + N_1(A, B)L(j\omega) = 0 \quad (10b)$$

To predict the limit cycles in all possible regions determined by the breakpoints, bias A , and the amplitude B of the of the limits cycles have been considered. To locate all possible limit cycles the solutions of $\sum_{p=1}^n \binom{n}{p}$ nonlinear equations in the form

$$1 + N_0^{(p,r)}(A, B)L(0) = 0 \quad (11a)$$

$$1 + N_1^{(p,r)}(A, B)L(j\omega) = 0 \quad (11b)$$

where $N_0^{(p,r)}, N_1^{(p,r)}$ are the gains of the nonlinearity which contains p breakpoints ($p = 1, 2, \dots, n$) including $\{S_{r+i} | i = 0, 1, \dots, p-1\}$ for $r = 1, 2, \dots, n-p+1$.

For the nonlinearity including p breakpoints in the region $S_{r-1} < y(t) < S_{r+p}$, $r = 1, 2, \dots, n-p+1$, the DIDFs have been obtained by using a symbolic solver for the generalized Chua's diode as,

$$\begin{aligned} N_0^{(p,r)}(A, B) &= \frac{1}{2A} [(m_{p+r} + m_r)A + k_{p+r} + k_r] \\ &+ \frac{1}{A\pi} \sum_{i=1}^p \left\{ [(m_{r+i} - m_{r+i-1})A + (k_{r+i} - k_{r+i-1})] \right. \\ &\quad \times \sin^{-1} \left(\frac{A - S_{r+i}}{B} \right) \\ &\quad \left. + (m_{r+i} - m_{r+i-1}) \sqrt{B^2 - (A - S_{r+i})^2} \right\} \end{aligned} \quad (12)$$

$$\begin{aligned} N_1^{(p,r)}(A, B) &= \frac{1}{2}(m_{p+r} + m_r) \\ &+ \frac{1}{\pi} \sum_{i=1}^p \left\{ (m_{r+i} - m_{r+i-1}) \sin^{-1} \left(\frac{A - S_{r+i}}{B} \right) \right. \\ &\quad \left. + \frac{(m_{r+i} - m_{r+i-1})(A + S_{r+i}) + 2(k_{r+i} - k_{r+i-1})}{B^2} \right. \\ &\quad \left. \times \sqrt{B^2 - (A - S_{r+i})^2} \right\} \end{aligned} \quad (13)$$

To interpret the bifurcation phenomena, the stability of the located limit cycles has to be considered. Assuming that the bias is constant for small perturbations, the stability of the Predicted Limit Cycles (PLC) can be studied via Loeb criteria [2, 6]. The relative location of the $-\frac{1}{N_1(A_0, B)}$ locus with respect to the amplitude B and the $L(j\omega)$ locus with respect to frequency ω provides the stability information of a limit cycle, and a sustained oscillation or a limit cycle occurs when $-\frac{1}{N_1(A_0, B)}$ locus and $L(j\omega)$ locus intersect. If $-\frac{1}{N_1(A_0, B)}$ is enclosed by the $L(j\omega)$ locus, then the system is unstable and the output amplitude subjected to any disturbance will increase, on the other hand if it is not enclosed the system is stable, then the output amplitude will decrease. Hence, by examining the locus in the range $|A - A_0| \leq \Delta A$ for the bias, the stability of predicted limit cycle can be concluded, where A_0 and B_0 are bias and amplitude of the PLC, respectively.

The instability of the PLC can also be verified analytically following the same line of reasoning in [2], which is stated for single sinusoidal input describing functions. The Eq. (10) can be represented as

$$U_0(A, B) = 0 \quad (14a)$$

$$U_1(A, B, \omega) + jV_1(A, B, \omega) = 0 \quad (14b)$$

Consider a small simultaneous perturbation in amplitude, bias and the frequency as

$$A \rightarrow A + \Delta A$$

$$B \rightarrow B + \Delta B$$

$$\omega \rightarrow \omega + \Delta\omega + j\Delta\sigma$$

where $\Delta\sigma \triangleq -\frac{dB}{B}$. And the perturbed solution should still satisfy Eq. (10). Hence,

$$U_0(A + \Delta, B + \Delta B) = 0 \quad (15a)$$

$$U_1(A + \Delta A, B + \Delta B, \omega + \Delta\omega + j\Delta\sigma) = 0 \quad (15b)$$

$$V_1(A + \Delta A, B + \Delta B, \omega + \Delta\omega + j\Delta\sigma) = 0. \quad (15c)$$

Taylor series expansion of Eq. (14), around the point (A, B, ω) rearranging and ignoring higher order terms yield to the first order,

$$\frac{\partial U_0}{\partial A} \Delta A + \frac{\partial U_0}{\partial B} \Delta B = 0 \quad (16a)$$

$$\begin{aligned} \frac{\partial U_1}{\partial \omega} \Delta\omega - \frac{\partial V_1}{\partial \omega} \Delta\sigma + \frac{\partial U_1}{\partial B} \Delta B + \frac{\partial U_1}{\partial A} \Delta A \\ + j \left(\frac{\partial V_1}{\partial \omega} \Delta\omega + \frac{\partial U_1}{\partial \omega} \Delta\sigma + \frac{\partial V_1}{\partial B} \Delta B + \frac{\partial V_1}{\partial A} \Delta A \right) = 0. \end{aligned} \quad (16b)$$

Eliminating $\Delta\omega$ in the real and imaginary parts of Eq.(16b) using the Eq.(16a) gives,

$$\begin{aligned} \left(\frac{\partial U_1}{\partial \omega} \right)^2 + \left(\frac{\partial V_1}{\partial \omega} \right)^2 = \frac{\Delta B}{\Delta\sigma} \left\{ \frac{\partial U_0}{\partial B} \left(\frac{\partial U_1}{\partial \omega} \frac{\partial V_1}{\partial A} - \frac{\partial V_1}{\partial \omega} \frac{\partial U_1}{\partial A} \right) \right. \\ \left. - \left(\frac{\partial U_1}{\partial \omega} \frac{\partial V_1}{\partial B} - \frac{\partial V_1}{\partial \omega} \frac{\partial U_1}{\partial B} \right) \right\}. \end{aligned} \quad (17)$$

In order that the PLC to be stable, the increment ΔB and $\Delta\sigma$ must have the same sign, i.e. $\Delta\sigma/\Delta B > 0$. Since the left hand side of Eq.(17) is always positive, it is necessary that,

$$\begin{aligned} \frac{\partial U_0}{\partial B} \left(\frac{\partial U_1}{\partial \omega} \frac{\partial V_1}{\partial A} - \frac{\partial V_1}{\partial \omega} \frac{\partial U_1}{\partial A} \right) \\ - \left(\frac{\partial U_1}{\partial \omega} \frac{\partial V_1}{\partial B} - \frac{\partial V_1}{\partial \omega} \frac{\partial U_1}{\partial B} \right) \Bigg|_{\substack{A=A_0 \\ B=B_0 \\ \omega=\omega_0}} > 0 \end{aligned} \quad (18)$$

for the predicted limit cycle to be stable, where A_0 , B_0 and ω_0 are bias, amplitude and frequency of the PLC, respectively.

The PLC (5) is said to be *interacting* with a equilibrium point $y(t) = E$, if,

$$B \geq \eta |A - E| \quad (19)$$

with $\eta \approx 1$ [3].

For the n-scroll case, one expects to find n PLCs interacting with one or more unstable equilibrium points, loosing their stabilities as the level of interaction increases (i.e. the distance between the equilibrium points and the PLCs decreases).

4. Computational Results

Since the nonlinearity is symmetric about the origin, examining the system for $y > 0$ will be sufficient. As an

example, for $\alpha = 9, \beta = 14.286$ and,

$$\phi(y) = \begin{cases} -0.143y, & 0 < |y| \leq 1 \\ 0.286y - 0.429 \text{ sign}(y), & 1 < |y| \leq 2.15 \\ -0.571y + 0.414 \text{ sign}(y), & 2.15 < |y| \leq 3.60 \\ 0.286y - 1.671 \text{ sign}(y), & 3.60 < |y| \end{cases}$$

have been chosen.

For the range $\delta \in (-1.000, -0.857)$, the circuit either exhibits limit cycles, single, double or 2-double scroll strange attractors. The computations indicate that there are several solutions satisfying the system of equations (11) for various regions. However, only the solutions for $(p, r) = (1, 1)$ and $(p, r) = (3, 1)$ are interacting with the unstable equilibrium point at the origin after a critical value of δ . These limit cycles cause the double scroll and the 2-double scroll behavior. The results for various values of δ , the solutions for these predicted limit cycles are summarized in Table 1 and 2.

The stability of predicted limit cycles is first examined using inequality (15). If the inequality (15) is true, the Loeb criteria is examined to determine the stability for a range of bias values centered around A_0 . For $\delta = -0.890$, both PLCs are far away from the origin and only $(p, r) = (1, 1)$ is stable. Increasing δ until -0.920 the situation does not change. The limit cycles loose their stability after $\delta = -0.925$. In simulations, it is observed that there exists a period-2 limit cycle at $\delta = -0.925$, and period-4 limit cycle, single scroll, double scroll and 2-double scroll with decreasing values of δ .

The level of interaction can be determined using the distance between the projection of the predicted limit cycle on the y -axis and unstable equilibrium point at the origin, i.e. $d = |A_0 - |B_0||$. When the bias A_0 and the amplitude B_0 values are examined, for decreasing values of δ , an increasing interaction with the unstable equilibrium point origin is observed. The limit cycle indicated by $(p, r) = (3, 1)$ is already in interaction with the origin around $\delta = -0.962$, and $(p, r) = (1, 1)$ limit cycle interacts with the origin around $\delta = 1$ (Fig. 2). This verifies that the 2-double scroll behavior is due to the interaction of four limit cycles with unstable equilibrium point.

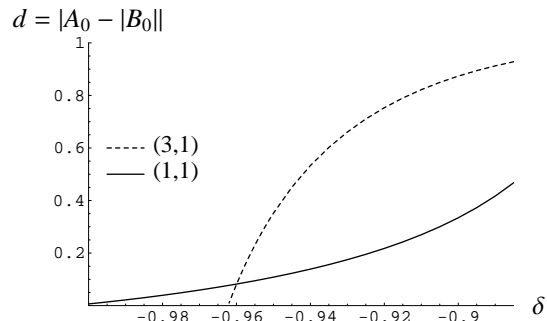


Figure 2: The level of interaction as the bifurcation parameter δ is varied.

Table 1: Bias A_0 , amplitude B_0 , frequency ω_0 of the PLC and the stability of the PLC for the regions $(p, r) = (1, 1)$

| δ | $\pm A_0$ | B_0 | ω_0 | η | Stability of the PLC | Simulation |
|----------|-----------|---------|------------|---------|----------------------|-----------------|
| -0.920 | 0.83814 | 0.62051 | 2.45069 | 0.78237 | stable | period-1 cycle |
| -0.940 | 0.86505 | 0.72618 | 2.45069 | 0.86115 | unstable | period-2 cycle |
| -0.945 | 0.87433 | 0.75136 | 2.45069 | 0.87703 | unstable | period-4 cycle |
| -0.950 | 0.88454 | 0.77627 | 2.45069 | 0.89173 | unstable | period-n cycle |
| -0.975 | 0.94892 | 0.90011 | 2.45069 | 0.95119 | unstable | single-scroll |
| -0.995 | 1.01652 | 1.00274 | 2.45069 | 0.98622 | unstable | double-scroll |
| -1.000 | 1.03580 | 1.02943 | 2.45069 | 0.99363 | unstable | 2 double-scroll |

Table 2: Bias A_0 , amplitude B_0 , frequency ω_0 of the PLC and the stability of the PLC for the regions $(p, r) = (3, 1)$

| δ | $\pm A_0$ | B_0 | ω_0 | η | Stability of the PLC | Simulation |
|----------|-----------|----------|------------|---------|----------------------|----------------|
| -0.920 | 4.39377 | -3.64057 | 2.45069 | 0.24680 | unstable | period-1 cycle |
| -0.940 | 4.37371 | -3.84064 | 2.45069 | 0.46693 | unstable | period-2 cycle |
| -0.945 | 4.34887 | -3.89809 | 2.45069 | 0.54922 | unstable | period-4 cycle |
| -0.950 | 4.31201 | -3.96034 | 2.45069 | 0.64833 | unstable | period-n cycle |
| -0.962 | 4.15296 | -4.14314 | 2.45069 | 0.99019 | unstable | single scroll |

5. Conclusions

In this paper, it has been shown that, it is possible to predict chaos in the generalized Chua's circuit exhibiting n -scroll attractors by harmonic balance analysis. To predict the interacting limit cycles, the dual input describing functions for n -break point nonlinearity has been derived. The stability of predicted limit cycles have been examined graphically and also an analytical necessary condition for the stability of the predicted limit cycles has been given. The interaction of the unstable equilibria with n -unstable predicted limit cycles is a strong indication of n -scroll chaos. The level of interaction has been measured using the distance between the interacting limit cycles and the equilibria. The usual period doubling route to chaos has been characterized by the increasing level of interaction.

References

- [1] L. O. Chua, M. Komuro, and T. Matsumoto. The double scroll family. *IEEE Transactions on Circuits and Systems*, 33:1072–1118, 1986.
- [2] Arthur Gelb and Wallace E Vander Velde. *Multiple-Input Describing Functions and Nonlinear System Design*. McGraw Hill, New York, U.S.A., 1967.
- [3] R. Genesio and A. Tesi. Harmonic balance methods for the analysis of chaotic dynamics in nonlinear systems. *Automatica*, 28(3):531–548, 1992.
- [4] T. Matsumoto. A chaotic attractor from Chua's circuit. *IEEE Transactions on Circuits and Systems*, 31:1055–1058, 1984.
- [5] Christian Mira. Chua's circuit and the qualitative theory of dynamical systems. *Journal of Franklin Institute*, 334B(5/6):737–744, 1997.
- [6] Katsuhiko Ogata. *Modern Control Engineering*. Prentice-Hall, New Jersey, U.S.A., 2nd edition, 1990.
- [7] F. A. Savacı, S. Günel, N. Özkurt, and I. İ. Yapalı. Harmonic balance analysis of generalizad chua's circuit. In *Intenational Conference on Progress in Nonlinear Science*, Nizhny Novgorod, Russia, 2001.
- [8] J. A. K. Suykens, A. Huang, and Leon O. Chua. A family of n -scroll attractors from a generalized Chua's circuit. *AEÜ International Journal of Electronic Communication*, 51(3):131–138, 1997.
- [9] J. A. K. Suykens and J. Vandewalle. Quasilinear approach to nonlinear systems and the design of n -double scroll ($n=1,2,3,4,\dots$). *IEEE Proceedings-G*, 138(5):595–603, 1991.
- [10] J. A. K. Suykens and J. Vandewalle. Generation of n -double scrolls ($n=1, 2, 3, 4,\dots$). *IEEE Transactions on Circuits and Systems I: Fundamental Theory and Applications*, 40(11):861–867, 1993.
- [11] M. E. Yalçın, S. Özoğuz, J. A. K. Suykens, and J. Vandewalle. 2d grid scroll attractors. In *Proceedings of NDES*, pages 181–184, The Netherlands, 2001.
- [12] M. E. Yalçın and F. A. Savacı. New realization of chua's Circuit and verification of chaos by harmonic balance analysis. *ARI - An International Journal for Physical and Engineering Sciences*, 51(3):169–174, 1999.
- [13] M. E. Yalçın, J. A. K. Suykens, and J. Vandewalle. Experimental comfirmation of 3- and 5-scroll attractors from a generalized Chua's circuit. *IEEE Transactions on Circuits and Systems-I*, 47(3):425–429, 2000.
- [14] Müştak E. Yalçın. *Cellular Neural Networks, Multi-Scroll Chaos and Synchronization: Theory, Applications and Implementations*. Ph.d. thesis, Katholieke Universiteit Leuven, Departement Elektrotechniek, Belgium, 2004.